

# We are IntechOpen, the world's leading publisher of Open Access books Built by scientists, for scientists

6,900

Open access books available

186,000

International authors and editors

200M

Downloads

Our authors are among the

154

Countries delivered to

TOP 1%

most cited scientists

12.2%

Contributors from top 500 universities



WEB OF SCIENCE™

Selection of our books indexed in the Book Citation Index  
in Web of Science™ Core Collection (BKCI)

Interested in publishing with us?  
Contact [book.department@intechopen.com](mailto:book.department@intechopen.com)

Numbers displayed above are based on latest data collected.  
For more information visit [www.intechopen.com](http://www.intechopen.com)



# Modeling and Optimization of Product Profiles in Biomass Pyrolysis

*Udaya Bhaskar Reddy Ragula, Sriram Devanathan  
and Sindhu Subramanian*

## Abstract

Biomass feed comes in many varieties, but have common chief constituents of hemicellulose, cellulose, and lignin. As the relative proportions of these constituents may vary, customization of the pyrolysis process conditions is required to produce a desired product profile. By recognizing the sources of variation, the reactor settings may be intelligently controlled, to achieve optimal operation. These considerations include biomass classification, feed rate, moisture content, particle size, and inter-particle thermal gradients (which arise during pyrolysis based on heating rate and temperature distribution). This chapter addresses the optimization of product profiles during biomass pyrolysis from a modeling perspective. Fundamental models for packed bed and fluidized bed pyrolyzers are developed, using kinetics from existing literature. The proposed optimization approach (inclusive of the kinetic and process models) can guide practical achievement of desired product profiles of the biomass pyrolysis process.

**Keywords:** biomass pyrolysis, product profiles, kinetics, modeling and optimization

## 1. Introduction

The chief constituents of any biomass are hemicellulose, cellulose, lignin and inerts [1]. The amounts of the chief constituents of various biomasses along with the elemental compositions are presented in **Table 1**. Generally, pyrolysis is a process where biomass or other carbonaceous material is heated in the absence of air supply or in the presence of inert gas supply such as nitrogen. During the biomass pyrolysis, the bonds between high molecular compounds are broken and low molecular weight compounds are formed. The range of pyrolysis products are gases, liquids, char, and ash. The ash is the inert material present in biomass. The fractions of these products depend on composition of biomass and process conditions such as heating rate, biomass feed rate, particle size, moisture content, and the rate of heat transfer. The rate of heat transfer depends greatly on mixing conditions in the pyrolyzers.

**Table 1** provides the chief constituents of biomass in wt% on dry and ash free basis along with the elemental composition for various biomasses. These chief constituents will vary depending on the type, location, and age of the plant. The error in values reported in **Table 1** is 2–5%. The wt% of hemicellulose varies from

Type of biomass	Biomass constituents			Elemental composition				Ref.#	
	HEMI* (%)	CEL* (%)	LIG* (%)	C (%)	H (%)	N (%)	S (%)		O (%)
Rice husk	19.1	44.6	36.3	39.8	5.7	0.5	0.2	39.8	[2]
Cotton stalk	23.5	48.2	28.4	46.8	6.4	0.3	0.2	46.8	[2]
Rice straw	28.5	54.5	17.0	38.8	6.7	0.2	0.2	38.8	[2]
Wheat straw	25.5	49.3	25.2	41.7	5	0.4	0.3	41.7	[2]
Corn stalk	52.9	28.0	19.1	43.8	5.7	0.9	0.1	48.9	[3]
Corn cob	35.4	47.0	17.7	43.6	5.8	0.7	1.3	48.6	[3]
Elephant grass	34.3	31.5	34.2	44.5	5.4	1.4	—	31.8	[3]
Hazelnut shell	17.4	25.4	57.2	52.3	6.5	5.2	9.2	26.8	[3]
Sugarcane bagasse	33.1	42.7	24.2	45.1	6.05	0.3	—	42.7	[3]
Switch grass	51.6	32.3	16.1	44.7	5.7	0.3	—	49.1	[4]
Hazelnut husk	22.8	38.2	38.9	42.6	5.5	1.1	0.1	50.6	[5]
Walnut shell	25.4	23.5	51.1	47.5	6.3	0.4	—	45.6	[6]
Pinewood waste	28.4	43.0	28.5	49.3	6	0.04	—	44.5	[7]
Apple pomace	27.8	47.5	24.7	47.9	6.6	0.7	—	37.4	[8]
Chestnut shells	23.3	32.6	44.0	48.1	5.4	0.6	—	45.7	[9]
Cherry stones	28.0	28.1	43.9	51.1	7.2	3	—	38.6	[9]
Grape seeds	22.9	16.9	60.2	51.5	6.3	1.7	—	40.3	[9]
<i>P. juliflora</i>	18.8	51.6	29.6	43.3	6.32	1.3	0.07	48.9	[10]
Cashew nut shells	18.6	41.3	40.1	58.3	7	0.7	0.06	32	[3, 11]
Coconut shell	27.9	40.3	31.9	53.9	5.7	0.1	0.02	39.4	[3, 11]
<i>Cagon grass</i>	28.8	50.9	20.4	44.3	5.6	0.8	0.09	49.0	[12]
Karanja fruit Hull	48.4	12.0	39.6	45.1	6.1	—	0.36	48.4	[13]
Cotton stalk	23.5	48.2	28.4	46.8	6.4	0.3	0.2	46.8	[2]
<i>Hibiscus rosa sinensis</i>	19.1	44.6	36.3	40–43	4.7–6.0	0.8–4.9	0.04–0.7	34–38	[14, 15]
<i>Nerium oleander</i>	23.5	48.2	28.4	44	6.7	0.5–1.2	0.04–0.2	30–35	[14, 16]

\*HEMI, hemicellulose; CEL, cellulose; LIG, lignin.

**Table 1.**  
Different biomasses, their constituents and elemental analysis.

17.4 to 52.9, the wt% of cellulose varies from 12 to 54.5% and the wt% of lignin varies from 16.1 to 60.2.

As shown in **Table 1**, there is significant variation across different biomasses. Thus, products resulting from biomass pyrolysis will also vary widely, and hence, it will be difficult to control the product profiles if enough attention is not paid to these chief constituents along with the biomass processing conditions.

This book chapter considers packed bed and fluidized bed pyrolyzers, which vary significantly in their heat transfer capabilities because of the mixing conditions. Section 2 of the chapter describes different pyrolysis processes and their associated product profiles. In view of their importance in pyrolysis, the reaction

kinetics are provided in Section 3. These kinetic parameters are obtained from a combination of prior published work and the authors' experimental data, based on thermogravimetric analysis (TGA) and lumped parameter models. Section 4 deals with the modeling of continuous packed bed and fluidized bed pyrolyzers, accounting for the variation in product profiles due to variation in feed and operating parameters. Section 5 introduces the optimization of product profiles for these two types of pyrolyzers under continuous operation.

## 2. Different pyrolysis processes

The primary products of the pyrolysis are gas, oil, char and water. The ratios of these products depend on parameters such as particle size, heating rate, degradation temperature, and feed rate of the material [14, 17–22]. The different pyrolysis processes are flash/fast pyrolysis, intermediate pyrolysis, and slow pyrolysis [1, 17, 20, 23–25]. The pyrolysis process is classified based on the heating rate as well as the degradation temperature of biomass. The operating parameters of different pyrolysis processes are given in **Figure 1**.

### 2.1 Flash/fast pyrolysis

Flash/fast pyrolysis is performed with very high heating rates ( $\sim 1000$  K/s) for less than a second. Since, the entire biomass particles are required to be heated for a very short time, only particles of very small size ( $< 1$  mm) can be pyrolyzed using this method. Because of small particle size and very short residence times, the thermal gradients within the particles are small, and hence, there is low product variation. This method is preferable if the number of components in the product stream is required to be low. With most of the biomasses during fast pyrolysis, the products are usually non-condensable gases.

### 2.2 Medium/intermediate pyrolysis

Intermediate pyrolysis is performed at medium heating rates. This kind of pyrolysis is preferred for biomass in the particle size range of 1–5 mm. During the intermediate pyrolysis, there are huge thermal gradients within the particle itself. Hence, intermediate pyrolysis is preferred when different products are required from the same biomass. Further, this type of reactor does not require a separate unit for product separation, especially, oil and water.

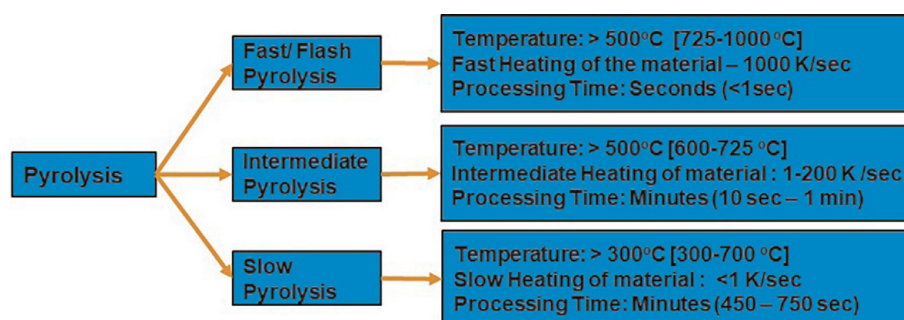


**Figure 1.**  
*Different types of pyrolysis and their operating conditions.*

## 2.3 Slow pyrolysis

Slow pyrolysis is performed at very low heating rates  $\sim 0.1$  K/s. The particle size during slow pyrolysis is between 2 and 10 mm. Slow pyrolysis is preferred if the charring characteristic of biomass is very high [4]. This is also the preferred type of pyrolysis when the residence time required during the pyrolysis is high.

Because of variations in the feed and the pyrolysis process, the thermal gradients are very high. Due to these thermal gradients within the particle and in the reactor, the reactions that the particles are undergoing are different, resulting in different product profiles. To design pyrolysis reactors with controlled product selectivity, it is important to understand which reactions are taking place in the reactor/biomass particle. This means that it is required to understand the kinetic parameters such as reaction order, activation energy, and pre-exponential factor for the reaction [14, 17, 23, 26–29]. Since, biomass particles are undergoing complicated reaction networks, the estimation of kinetic parameters were limited to the overall process in the early stages. Later, the kinetic parameters were estimated using the staged decomposition of biomass due to its chief constituents of biomass, namely, hemicellulose, cellulose, and lignin, and their relative proportions in a biomass [11, 14, 20, 30]. In the next section of this chapter, the kinetics of different biomasses are presented along with their corresponding parameters.

## 3. Pyrolysis kinetics and product profiles

Kinetics play an important role in the design of pyrolysis reactors. These kinetic parameters depend on the type of the biomass feed, mixing conditions in the reactor, and inter-particle & intra-particle thermal and mass transfer limitations. As mentioned earlier, the biomass pyrolysis consists of complicated reaction networks, making it difficult to analyze the pyrolysis kinetic parameters for individual reactions.

### 3.1 Pyrolysis kinetics

Different kinetic models were proposed by several authors working on the kinetics of the pyrolysis of biomass. Currently, there is no single model for the evaluation of kinetic parameters primarily based on the thermogravimetric (TGA) studies. The different types of kinetic models tested for the biomass pyrolysis are: (1) isoconversion (ISO) models such as Kissinger-Akahira-Sunose (KAS) model and Ozawa-Flynn-Wall (OFW) model, (2) generalized  $n^{\text{th}}$  order reaction model, (3) Coats-Redfern (CR) model, (4) three component mechanism with CR model, (5) Gaussian Distributed Activation Energy model (Gaussian DAEM), (6) Friedmann model, and (7) Starink model. The differences lie in their approach to relate them to rate of biomass degradation with kinetic parameters-mainly the activation energy and the pre-exponential factor.

The different models to analyze the pyrolysis thermal degradation data, were classified mainly into three categories namely, accelerating, decelerating, and sigmoidal model based on the shape of rate of degradation vs. time [17, 29]. The accelerating models are the ones whose rate of decomposition increases with the increase in time. For those biomasses which fall under this category a simple power law model with respect to rate of decomposition is more suitable [29]. The decelerating models are used whose rate of reaction decreases with increase in time, such as CR model and integral models (such as KAS and OFW models). This means, there are mass transfer limitations (diffusion limited) during the reaction due to the formation of products or inert layers that slows down the reaction. The sigmoidal models

Type of biomass	Model	Activation energy- $E_a$ (kJ/mol)	Pre-exponential factor-A ( $\text{min}^{-1}$ )	Reference
Rice husk	Gaussian DAEM	85–110	$10^5$ – $10^7$	[31]
Cotton stalk	Direct method	Hemicellulose: 102.0 Cellulose: 98.5	1.22 0.45	[32]
	Integral method	Hemicellulose: 127.8 Cellulose: 72.5	2.6 0.35	
Rice straw	Kissinger model	172.6	$10^{11}$	[32]
	OFW model	192.7	$10^{22}$	
	KAS model	193.6	$10^{15}$	
Wheat straw	nth-order reaction model	Cellulose and hemicellulose: 78 (n-0.65) Lignin: 80 (n-2.7)	$10^7$ $10^6$	[33]
Corn stalk	KAS model	62.7	$10^7$ – $10^8$	[34]
Corn cob	CR model	64–80	$10^3$	[35]
Switch grass	KAS model	77.4	$10^8$ – $10^9$	[34]
Elephant grass	Three component mechanism	Hemicellulose: 46.5– 65.5 Cellulose: 108–127.2 Lignin: 45.6–53.5	$10^4$ – $10^6$ $10^8$ – $10^{11}$ $10^2$ – $10^3$	[36]
Hazelnut husk	KAS model	127.8	—	[37]
	OFW model	131.1	—	
	CR model	—	$10^5$ – $10^6$	
Hazelnut shell	Friedman model	222.3	—	[38]
	KAS model	216.3	—	
	DE Algorithm	First zone: 35–153	$10^{-3}$ – $10^8$	
	CR model	Second zone: 20–135 35.9	$10^{-4}$ – $10^6$ $10^2$	
Walnut shell	Arrhenius model	69.3	$10^5$	[6]
	CR model	101.6	$10^5$	
Pine wood	Arrhenius model	150	$10^{11}$	[39]
Apple pomace	Friedman model	197.7	—	[8]
	OFW model	213.0	—	
	KAS model	201.7	—	
	CR model	—	$10^{-1}$ – $10^{-3}$	
Chestnut shells	Friedman model	127.2–194.8	—	[40]
	KAS model	152.7–196.7	—	
	OFW model	154.1–196.1	—	
	Starink model	153.2–196.9	—	
	DAEM	175.2	$10^{11}$ – $10^{15}$	
Cherry stones	Arrhenius equation	Hemicellulose: 197.7	$10^{10}$	[41]
		Cellulose: 213.0	$10^7$	
		Lignin: 201.7	$10^2$	
Grape seeds	Gaussian DAEM	$188 \pm 3$	$10^{-2}$	[42]
	Logistic DAEM	$190 \pm 2$	$10^{-2}$	
<i>P. juliflora</i>	KAS model	204.0	$10^{11}$	[10]
	OFW model	203.2	$10^5$	
	Friedman model	219.3	$10^{21}$	
Sugarcane bagasse	Direct method	Hemicellulose: 53.5, cellulose: 43	$10^{-1}$ $10^{-1}$	[32]
	Integral method	Hemicellulose: 87.7, cellulose: 77	$10^{-1}$ $10^{-1}$	

Type of biomass	Model	Activation energy- $E_a$ (kJ/mol)	Pre-exponential factor-A ( $\text{min}^{-1}$ )	Reference
Cashew nut shells	CR model	Hemicellulose: 130.2 Cellulose: 174.3	$10^{-1}$ - $10^{-4}$ $10^{-2}$ - $10^{-3}$	[11]
Coconut shell	CR model	Hemicellulose: 179.6 Cellulose: 216.0	$10^{-1}$ - $10^{-5}$ $10^{-1}$ - $10^{-3}$	[11]
Imperata cylindrical (Cagon grass)	DAEM Global kinetic model	213.9 60-64	$10^{13}$ $10^1$ - $10^2$	[12]
Karanja fruit Hull	KAS model OFW model	61.0 68.5	$10^6$ $10^6$	[13]
<i>Hibiscus rosa sinensis</i>	CR model	Hemicellulose: 55-91 Cellulose: 9-62 Lignin: 65-142	$10^6$ - $10^8$ $10^{-1}$ - $10^3$ $10^4$ - $10^7$	[14]
<i>Nerium oleander</i>	CR model	Hemicellulose: 29-51 Cellulose: 11-43 Lignin: 71-109	$10^2$ - $10^4$ $10^{-1}$ - $10^3$ $10^2$ - $10^5$	[14]

**Table 2.**  
Kinetic parameters of pyrolysis of different biomasses.

represent the autocatalytic type reactions during biomass pyrolysis, such as OFW and KAS models. The choice of the kinetic model purely depends on the rate of decomposition vs. time curve.

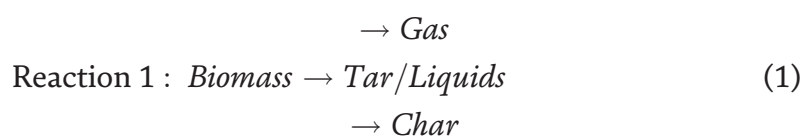
The isoconversion model and Gaussian DAEM will give only the activation of energy for the overall thermal degradation process, which is further used in Arrhenius type model for finding the pre-exponential factor.

**Table 2** provides the kinetic parameters reported by researchers for different biomasses that are widely used in pyrolysis.

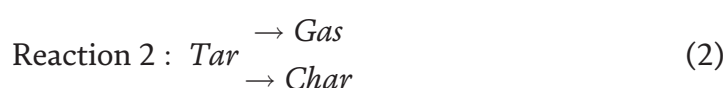
Comparing **Tables 1** and **2**, for the biomasses with high hemicellulose content, the activation energy is between 50 and 65 kJ/kmol, and the pre-exponential factor is between  $10^3$  and  $10^8 \text{ min}^{-1}$ . The activation energy for high cellulose content is between 170 and 220 kJ/kmol and the pre-exponential factor is between  $10^7$  and  $10^{21} \text{ min}^{-1}$ . For the biomasses with high lignin content, the activation energy ranges from 65 to 140 kJ/kmol and the pre-exponential factor ranges from  $10^{-1}$  to  $10^7 \text{ min}^{-1}$ . These wide variations in the kinetic parameters indicate that different reactions are occurring within the biomass particle.

### 3.2 Pyrolysis product profiles: lumped product distribution

It has been mentioned earlier that the products of biomass pyrolysis vary widely. There are not many studies aimed at intrinsic kinetic parameter estimation for each individual products of pyrolysis. The pyrolysis products are lumped based on their standard phase. The lumped reaction model for the biomass pyrolysis is given in Eqs. (1) and (2) [43, 44].



The tar formed during the primary biomass decomposition shall further decompose into gas and char.



Biomass type	Pyrolysis type	Pyrolysis conditions	Reactor type	Products (wt%)	Ref #
Rice husk	Intermediate	Temp.: >500°C HR: >3.33 K/s Size: <0.5 mm	Fluidized bed	Gas: 15% Liquids: 37–40% Char: 47%	[45]
	Slow	Temp.: >500°C HR: >0.33 K/s Size: <0.21 mm	Fixed bed	Gas: 32.7% Liquids: 30.1% Char: 31.8%	[46]
Cotton stalk	Intermediate	Temp.: 490°C HR: 9 K/s Size: 1 mm	Fluidized bed	Gas: 23% Liquids: 36% Char: 16%	[47]
	Slow	Temp.: 600°C HR: 0.3 K/s Size: 3 mm	Fixed bed	Gas: 44.8% Liquids: 17.1% Char: 38%	[24, 48]
Rice straw	Intermediate	Temp.: 500°C HR: 3.3 K/s Size: <0.5 mm	Fixed bed	Gas: 54% Liquids: 6% Char: 40%	[20]
	Slow	Temp.: 600°C HR: 0.16 K/s Size: 0.3 mm	Fixed bed	Gas: 30% Liquids: 45% Char: 28%	[49, 50]
Wheat straw	Fast/flash	Temp.: 525°C HR: 250–1000 K/s Size: 0.25–1 mm	Fluidized bed	Gas: 26.9% Liquids: 34.9% Char: 28.0%	[28]
	Slow	Temp.: 450°C HR: 0.03 K/s Size: 1.33 mm	Fixed bed	Gas: 24% Liquids: 34% Char: 43%	[51]
Corn stalks	Intermediate	Temp.: 500°C HR: 8.3 K/s Size: <0.5 mm	Fluidized bed	Gas: 35% Liquids: 38% Char: 28%	[52]
	Slow	Temp.: 400°C HR: 0.83 K/s Size: <1 mm	Fixed bed	Gas: 12% Liquids: 50% Char: 38%	[53]
Corn cob	Fast/flash	Temp.: 550°C HR: 1000 K/s Size: 1–2 mm	Fluidized bed	Gas: 46% Liquids: 36% Char: 18%	[54]
	Intermediate	Temp.: 577°C HR: 10 K/s Size: 0.5–2 mm	Fixed bed	Gas: 49% Liquids: 28% Char: 23%	[55]
Elephant grass	Fast/flash	Temp.: 480–520°C HR: 4000 K/s Size: 0.8–1.2 mm	Fluidized bed	Gas: 36.3% Liquids: 37.6% Char: 27.8%	[56, 57]
	Slow	Temp.: 500°C HR: 0.16 K/s Size: 0.21 mm	Fixed bed	Gas: 26% Liquids: 44.7% Char: 29.3%	[58]
Hazelnut shell	Slow	Temp.: 550°C HR: 0.1 K/s Size: 0.85–1.8 mm	Fixed bed	Gas: 21.5% Liquids: 22.5% Water: 25% Char: 31%	[59]
	Intermediate	Temp.: 550°C HR: 5 K/s Size: 0.85–1.8 mm	Fixed bed	Gas: 27% Liquids: 34% Water: 11% Char: 28%	[59]
Sugarcane bagasse	Intermediate	Temp.: 500°C HR: 3.3 K/s Size: <0.5 mm	Fixed bed	Gas: 55% Liquids: 10% Char: 35%	[20]
	Slow	Temp.: 420°C HR: 0.35 K/s Size: <0.5 mm	Fixed bed	Gas: 24.4% Liquids: 43% Char: 32.6%	[60]

Biomass type	Pyrolysis type	Pyrolysis conditions	Reactor type	Products (wt%)	Ref #
Switch grass	Fast/flash	Temp.: 510°C HR: 1000 K/s Size: 0.25–1 mm	Fluidized bed	Gas: 16.5% Liquids: 57.9% Char: 20.0%	[28]
	Slow	Temp.: 500°C HR: 0.17 K/s Size: 0 < 1 mm	Fixed bed	Gas: 43.2% Liquids: 27.5% Char: 29.3%	[61]
Walnut shell	Intermediate	Temp.: 500°C HR: 5 K/s Size: 0.6–1.8 mm	Fixed bed	Gas: 15.6% Liquids: 31% Char: 27.5%	[62]
	Slow	Temp.: 550°C HR: 0.16–1 K/s Size: 0.075 mm	TGA	Gas: 10% Liquids: 25% Char: 40%	[63]
Pine wood	Fast/flash	Temp.: 400–500°C HR: >1000 K/s Size: 0.25–0.425 mm	Fluidized bed	Gas: 22% Liquids: 67% Char: 11%	[64]
	Intermediate	Temp.: 500°C HR: 5 K/s Size: 0.6–0.85 mm	Fixed bed	Gas: 26% Liquids: 43% Char: 23% Water: 14%	[65]
	Slow	Temp.: 700°C HR: 0.16 K/s Size: <1 mm	Fixed bed	Gas: 25% Liquids: 58% Char: 18%	[66]
Apple pomace	Slow	Temp.: 400°C HR: 0.08–0.3 K/s Size: 420–840 µm	Fixed bed	Gas: 71.5% Liquids: 25.4% Char: 3%	[23]
Coconut shell	Intermediate	Temp.: 500°C HR: 3.3 K/s Size: <0.5 mm	Fixed bed	Gas: 51% Liquids: 10% Char: 39%	[20]
	Slow	Temp.: 550°C HR: 1 K/s Size: 1.18–1.8 mm	Fixed bed	Gas: 30–33% Liquids: 38–44% Char: 22–31%	[67]
Cashew nut shells	Slow	Temp.: 400–450°C HR: 0.166 K/s Size: 0.25 mm	Fixed bed	Gas: 57.4% Liquids: 23.5% Char: 19.1%	[68]
Cherry stones	Slow	Temp.: 400–500°C HR: 0.083–0.33 K/s Size: 0.32–2 mm	TGA	Gas: 8.8–47.6% Liquids: 32–58% Char: 20–56.8%	[41]
<i>P. juliflora</i>	Fast/flash	Temp.: 450°C HR: >4000 K/s Size: 0.25–0.5 mm	Fluidized bed	Gas: 12.5% Liquid: 62.5% Char: 25%	[57, 69]
	Slow	Temp.: 600°C HR: 0.33 K/s Size: 0.2–0.5 mm	Fixed bed	Gas: 44% Liquid: 38.3% Char: 36.8%	[70]
<i>Cogon grass</i>	Slow	Temp.: 500°C HR: 0.36 K/s Size: 0.25–1 mm	Fixed bed	Gas: 49.1–74.1% Oil: 3.2–20.8% Char: 22.6–30.5%	[12]

Temp., temperature; HR, heating rate; size, biomass particle size.

**Table 3.**

Product profiles from pyrolysis of different biomass in fixed and fluidized bed pyrolyzers.

For practical purposes, the products are classified into gases, liquids, and char. The lumped product distribution from pyrolysis of different biomasses, different pyrolysis methods, pyrolysis conditions and two different pyrolyzers (fixed bed and fluidized) are provided (Table 3).

From the data presented in **Table 3**, it can be generalized that the liquid products will be more in fluidized bed reactors, whereas more char is seen in fixed bed reactors. Further, slow pyrolysis results in more gas and char when compared to fast pyrolysis. This might be due to the liquid products formed in reaction 1, shown in Eq. (1), being further consumed by reaction 2, shown in Eq. (2) resulting in more gas and char. The relative proportions of these products depend on various parameters mentioned earlier.

#### 4. Process modeling of pyrolysis reactors

The biomass pyrolysis has been mainly carried out in two types of reactors: fixed bed (or packed bed) reactors and fluidized bed reactors, by many authors, as presented in **Table 3**. The process models for these two reactors are developed from fundamental laws of conservation of mass and energy along with empirical relations for properties such as specific heat, density, diffusivity, mass and heat transfer coefficients, etc. The packed bed pyrolyzers are further classified as down-draft and updraft pyrolysis reactors. The detailed comparison of the general packed bed and fluidized bed reactors is given in **Table 4**.

The biomass usually contains moisture. The moisture needs to be removed before the pyrolysis stage. If this is carried to the pyrolysis stage, the gasification reactions such as steam reformation may kick off resulting in undesirable products.

Gasifier type	Specifications/conditions
Updraft fixed bed pyrolyzer	<ul style="list-style-type: none"> <li>• The biomass is fed from the top of the pyrolyzer, and the inert gas (if any) fed from bottom.</li> <li>• Char resulting from pyrolysis falls down and may accelerate the pyrolysis.</li> <li>• The pyrolysis gases and along with the liquid tar (in the form of gas) leaves from the top of the pyrolyzer.</li> <li>• The ash (inert component of the biomass) is collected at the bottom of the gasifier.</li> <li>• Operating temperature ranges from 300 to 750°C.</li> </ul>
Downdraft fixed bed pyrolyzer	<ul style="list-style-type: none"> <li>• The biomass is fed from top of the pyrolyzer along with inert gas allowing the feed and gases move in the same direction.</li> <li>• The feed is broken down, falling down the gasifier under gravity. A bed of hot char through which the gases are allowed to pass through (a secondary reaction zone) ensures the pyrolysis products travelling from top are further broken down. This increases the residence time through the pyrolysis stage. An exit for the pyrolysis products is provided just above the bottom of the pyrolyzer.</li> <li>• The ash collected under the grate at the bottom the pyrolyzer.</li> <li>• Operating temperature ranges from 300 to 750°C.</li> </ul>
Fluidized bed reactor	<ul style="list-style-type: none"> <li>• A bed of fine inert solid material is present at the bottom of the pyrolyzer. The inert gas is fed from the bottom of the pyrolyzer fast enough (1–3 m/s) to agitate the material.</li> <li>• The biomass feed is fed in from the side, mixes with the inert gas and the products of the pyrolysis leave from the top.</li> <li>• The operating temperature is below 900°C to avoid ash melting and sticking to the wall.</li> </ul>

**Table 4.**  
*Comparison of fixed bed and fluidized bed pyrolyzers.*

The modeling of the packed bed and the fluidized bed pyrolyzers is discussed in detail below.

The major difference between the updraft pyrolyzer and the downdraft pyrolyzer is only the inlet and outlet locations, which changes the residence time and mixing conditions. For the purpose of the modeling of biomass pyrolysis and optimization of product profiles, the updraft and downdraft pyrolyzers are treated as fixed bed pyrolyzers.

#### 4.1 Modeling of packed bed pyrolysis reactor

The modeling of the packed bed pyrolysis reactors is divided into drying stage and the pyrolysis stage. The modeling of these two stages has been presented in detail below.

##### 4.1.1 Modeling of drying stage in packed bed pyrolyzers

The drying of biomass particles will happen in two stages: (a) constant rate period and (b) falling rate period. The rate of drying in these two stages is given separately by the following equations.

The rate of drying during the constant rate period is given by [71]

$$\frac{dX}{dt} = -k_c = 1.3 \times 10^{-9} T_g^{4.112} v_g^{0.219} \quad (3)$$

The rate of drying during the falling rate period is given by [71]

$$\begin{aligned} \frac{dX}{dt} &= -K(X - X_{eq}) \\ K &= 0.011 \exp(-201.8/T_g) \end{aligned} \quad (4)$$

Eqs. (3) and (4), provide an estimation of rate of drying in both constant and falling rate periods, with rate of drying depending on the particle temperature. During the pyrolysis process, the biomass particle temperature depends on the rate of heat transfer between the gas and the particle. This rate of heat transfer depends on the flow characteristics involving Reynolds and Prandtl number. For  $20 < Re < 1000$ , the heat transfer coefficient is given by [71, 72]

$$\begin{aligned} h &= 3.26 C_{pg} G_g Re^{-0.65} Pr^{2/3} \\ Re_p &= \frac{\rho_{gas} U_o d_p}{\mu} \end{aligned} \quad (5)$$

where  $k_c$  is the mass transfer coefficient at constant drying period in  $s^{-1}$ ;  $K$  is the mass transfer coefficient at falling drying period in  $s^{-1}$ ;  $Re$  is the Reynolds number of gas;  $Pr$  is the Prandtl number of gas;  $T_g$  is the gas temperature in  $^{\circ}C$ ;  $v_g$  is the gas velocity in  $m/s$ ;  $C_{pg}$  is the heat capacity of gas in  $J/(kg K)$ ;  $\epsilon_{mf}$  is the porosity at minimum fluidization;  $X$  is the moisture content in the biomass;  $X_{eq}$  is the moisture content at the end of constant rate period;  $G_g$  is the gas mass flux in  $kg/(m^2 s)$ .

##### 4.1.2 Modeling of pyrolysis in packed bed reactors

Eqs. (1) and (2) represents the reactions reported during pyrolysis of biomass with lumped product approach. Since the reaction presented in Eq. (1) involves

only the solid biomass as reactant, most of the reactions are treated as first order reactions using Arrhenius type model [73]. The Arrhenius model parameters for the lumped reaction model that produces gaseous, liquid, and char for different constituent of biomass are given in **Table 5**.

The volume and the moles of the products of the pyrolysis zone was found with the help of the plug flow reactor (PFR) design equation.

$$\frac{V}{F_{Biomass}} = \int_0^{X_f} \frac{dX_{Biomass}}{-r_{Biomass}} \quad (6)$$

$$(-r_{Biomass} = r_{Gas} + r_{Liquids} + r_{Char})$$

where  $V$  is the volume of the pyrolyzer in l,  $F_{Biomass}$  is the molar feed rate of biomass in mol/s;  $X_f$  is the desired biomass conversion;  $-r_{Biomass}$  is the rate of biomass consumption in mol/(lit. s);  $r_{Gas}$  is the rate of formation of gaseous products in mol/(lit. s);  $r_{Liquids}$  is the rate of formation of liquid products in mol/(lit. s);  $r_{Char}$  is the rate of formation of char in mol/(lit. s).

Since, the pyrolysis stage is non-isothermal in nature, it is essential to model the temperature along the length of the pyrolyzer which involves external heating. The energy balance equation was obtained based on the shell energy balance to find the temperature profile along the length of the pyrolysis zone. The steady state energy balance equation results in the following differential equation:

$$k \frac{d^2T}{dr^2} - \rho C_p v_z \frac{dT}{dz} + \frac{\epsilon_R}{R} \sigma (T_W^4 - T^4) - \Delta H_{RF_{AOD}} dX_A = 0 \quad (7)$$

where  $k$  is the thermal conductivity in W/(m. K);  $\rho$  is the density in kg/m<sup>3</sup>;  $C_p$  is the specific heat capacity in J/(kg. K);  $v_z$  is the gas velocity in m/s;  $\epsilon_R$  is the emissivity of the body during radiation;  $\sigma$  is the Stephan-Boltzmann constant = 5.67E-08 W/(m<sup>2</sup> K<sup>4</sup>);  $R$  is the radius of oxidation zone in m;  $T_W$  is the source temperature in K;  $T$  is the reactor temperature in K;  $r, z$  are the radial and axial directions.

Since, Eq. (7) is combined convection diffusion equation with heat source (heat of reaction) and external heat supply, two boundary conditions are required: one in radial direction and one in axial direction.

The boundary conditions for solving the energy balance equation are:

$$\begin{aligned} @r = R, k \frac{dT}{dr} &= \text{Radiation flux} \\ @r = 0; k \frac{dT}{dr} &= 0 \text{ (Temperature minimum condition)} \\ @z = 0; T &= T_o \end{aligned}$$

Pyrolysis product→	Gas		Tar/liquids		Char	
	A (s <sup>-1</sup> )	E <sub>a</sub> (J/mol)	A (s <sup>-1</sup> )	E <sub>a</sub> (J/mol)	A (s <sup>-1</sup> )	E <sub>a</sub> (J/mol)
HEMI*	2.1 × 10 <sup>16</sup>	1.8 × 10 <sup>5</sup>	8.7 × 10 <sup>14</sup>	2.0 × 10 <sup>5</sup>	2.6 × 10 <sup>11</sup>	1.5 × 10 <sup>5</sup>
CEL*	2.8 × 10 <sup>19</sup>	2.4 × 10 <sup>5</sup>	3.3 × 10 <sup>14</sup>	1.9 × 10 <sup>5</sup>	1.3 × 10 <sup>10</sup>	1.5 × 10 <sup>5</sup>
LIG*	9.6 × 10 <sup>8</sup>	1.1 × 10 <sup>5</sup>	1.5 × 10 <sup>9</sup>	1.4 × 10 <sup>5</sup>	7.7 × 10 <sup>6</sup>	1.1 × 10 <sup>5</sup>

\*HEMI, hemicellulose; CEL, cellulose; LIG, lignin.

**Table 5.**  
 Kinetic parameters for lumped models for biomass pyrolysis.

## 4.2 Modeling of fluidized bed pyrolysis reactor

As mentioned in the modeling of the packed bed pyrolysis, the pyrolysis process occurs after the drying of the biomass.

### 4.2.1 Modeling of drying stage in fluidized bed pyrolyzers

The equations for the drying stage in a fluidized bed pyrolyzers are similar to those in a packed bed pyrolyzer, as provided in Section 4.1.1. Because there is vigorous mixing in the fluidized bed pyrolysis, the extent of heat and mass transfer is very high. Kunii and Levenspiel confirmed that there is more than one phase during bubbling fluidization [74]. These two phases are named as bubble phase (primarily the fluid used as fluidizing the medium) and emulsion phase (mixture of biomass particles and fluid). The interface between these two phases is named as “cloud.” The concept of two-phase model along with the mass transfer between the two phases is depicted in **Figure 2**. It is to be noted that the primary reactions during biomass pyrolysis shall occur only in the solid phase (i.e., in the emulsion phase) and the secondary reactions occur in both phases.

The most widely used Kunii and Levenspiel model (K-L model) expresses the overall heat and mass transfer coefficient in a bubbling fluidized bed considering the resistance for heat and mass transfer between the bubble-cloud interface and resistance for heat and mass transfer between emulsion and cloud [74]. The cloud-bubble interface heat and mass transfer are functions of gas velocity and conduction/diffusion from a thin cloud layer into the bubble. The emulsion and cloud transfer are only due to conduction/diffusion between the emulsion phase and the cloud boundary. They had also suggested additional mass transfer resulting from particles dispersed in the bubbles. However, recent advanced imaging technique, have shown bubble free particles in most cases.

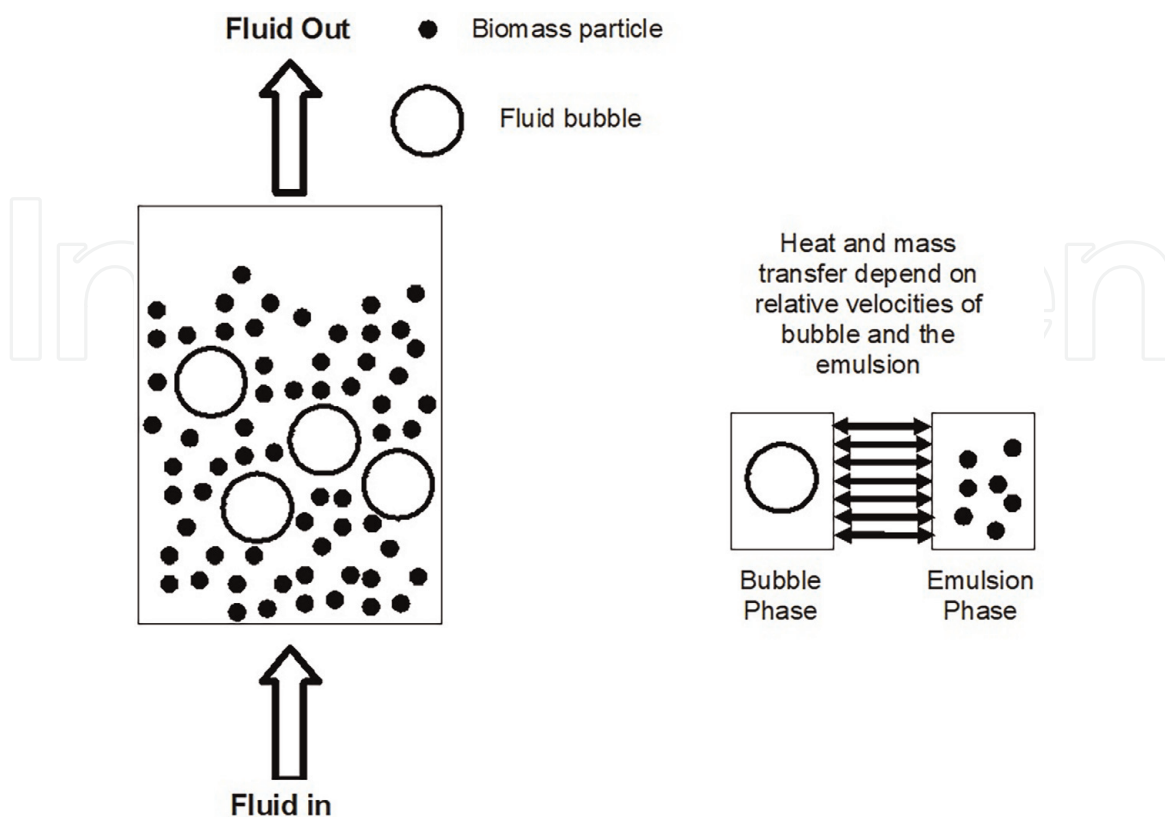


**Figure 2.**  
The two-phase model for fluidized bed pyrolyzer.

Based on the two-phase model, the overall mass transfer coefficient is estimated using Eqs. (8)–(10) [75].

**Cloud-bubble mass transfer coefficient**

$$k_{cb} = 1.5 \frac{U_{mbf}}{d_b} + 5.85 \left( \frac{D_{AB}^{0.5} g^{0.25}}{d_b^{1.25}} \right) \quad (8)$$

**Dense-cloud mass transfer coefficient**

$$k_{dc} = 6.77 \left( \frac{D_{AB} \varepsilon_{mf} U_b}{d_b^3} \right) \quad (9)$$

**Overall mass transfer coefficient (in s<sup>-1</sup>)**

$$\frac{1}{k_{overall}} = \frac{1}{k_{cb}} + \frac{1}{k_{dc}} \quad (10)$$

The heat transfer coefficient is estimated using the correlation given in Eq. (11) [76].

$$h_c = 0.15 \frac{k_g}{d_p} \text{Re}_p^{0.35} \text{Ar}^{0.25} (V_{gas} \leq U_o) \quad (11)$$

$$\text{Re}_p = \frac{\rho_{gas} U_o d_p}{\mu} \quad (12)$$

$$\text{Ar} = \frac{d_p^3 \rho_{gas} (\rho_{solid} - \rho_{gas}) g}{\mu^2} \quad (13)$$

where  $k_{dc}$  is the mass transfer coefficient between dense emulsion and cloud in m/s;  $k_{cb}$  is the mass transfer coefficient between bubble and cloud in m/s;  $k_{overall}$  is the overall mass transfer coefficient between bubble and cloud in m/s;  $h_c$  is the overall heat transfer coefficient in W/(m<sup>2</sup> K);  $\text{Re}_p$  is the Particle Reynolds number;  $\text{Ar}$  is the Archimedes number;  $U_{mbf}$  is the bubble velocity at minimum fluidization in m/s;  $D_{AB}$  is the binary diffusivity in m<sup>2</sup>/s;  $U_b$  is the bubble velocity in m/s;  $\varepsilon_{mf}$  is the bed voidage at minimum fluidization;  $\rho_{solid}$  is the density of biomass particle in kg/m<sup>3</sup>;  $\rho_{gas}$  is the density of fluidizing gas in kg/m<sup>3</sup>;  $d_b$  is the bubble diameter in m.

**4.2.2 Modeling of pyrolysis stage in fluidized bed pyrolyzers**

Due to vigorous mixing in the fluidized beds, the following assumptions are made for modeling of the pyrolysis stage in the fluidized bed reactors:

1. Isothermal operation of the reactor,
2. No radial variations, and
3. Reactions occurring only in the solid phase (only in the emulsion phase).

Based on these assumptions, the following models (separately for emulsion phase and bubble phase) can be obtained from the fundamental component balance:

$$\text{Bubble phase : } \varepsilon u_b \frac{dC_{A,b}}{dz} - k_L(C_{A,b} - C_{A,e}) = 0 \quad (14)$$

$$\text{Emulsion phase : } (1 - \varepsilon)u_e \frac{dC_{A,e}}{dz} + k_L(C_{A,b} - C_{A,e}) - (1 - \varepsilon)D_{eff} \frac{d^2C_{A,e}}{dz^2} + (-r_A)\rho_e(1 - \varepsilon) = 0; \quad (15)$$

where  $b$  is the bubble phase and  $e$  is the emulsion phase.

## 5. Optimization of product profiles in biomass pyrolysis

As discussed in Section 1, since the product profiles of biomass pyrolysis are known to greatly depend on various parameters, it is necessary to determine the parameters that have the largest effect on the ratios of important lumped products discussed in Section 2.

### 5.1 Response surface optimization methodology: the mixture design

The following quantifiable factors were chosen for the optimization. The biomass-based factors are:

- a. Hemicellulose fraction
- b. Cellulose fraction
- c. Lignin fraction

The process-based parameters have been divided into two categorical type parameters.

- a. The type of pyrolysis-slow and fast/flash pyrolysis
- b. The type of reactor-fixed bed and fluidized bed reactors

The variation of constituent composition of biomass is obtained from **Table 1**. The amounts of gaseous, liquid, and products for each biomass for different process parameters and different reactor types are obtained from **Table 3**.

Since hemicellulose, cellulose, and lignin are biomass constituents, the sum of their fractions must be equal to one. Accordingly, a mixture design was chosen for the statistical design of the experiments.

A total of 52 data sets were selected combining **Tables 1** and **3** (based on the variations in mixture design), and the experiments conducted and data analyzed.

The depletion of fossil fuels has created interest in obtaining the fuels from alternate sources such as biomass, especially for transportation fuels. Therefore, the objective of the product profiles from biomass pyrolysis is aimed to maximize the liquid (tar) products and simultaneously minimize the production of gas and char. The reason for the minimization of gaseous products is that they may contain carbon monoxide and carbon dioxide which are of less calorific value when compared to the hydrocarbons.

Ternary diagrams are common in representing factor levels in a mixture design. In such a diagram, with three factors ( $x_1$ ,  $x_2$ , and  $x_3$ ), the vertex represents a pure

component (i.e.,  $x_1 = 100\%$ ) while its opposite edge holds a value of  $x_1 = 0$  (with  $x_2 + x_3 = 100\%$ ). The same holds for the other two vertices and edges.

However, it may be noted that in certain experiments the sum of proportions of the three components may be deliberately constrained to equal a specific value. This feature has been used in our experimental design. For example, referring to **Figure 3**, the three vertices represent hemicellulose, cellulose and lignin. The maximum fraction of these three constituents is 0.764, 0.742 and 0.7444 for hemicellulose, cellulose and lignin, respectively. The 0.119, 0.117, and 0.139 marked on the sides of the triangle represent the minimum values for the biomass constituents.

## 5.2 Optimization of gas yield

The analysis of minimization of gas yield is separated into two types: (a) fast pyrolysis in fluidized bed pyrolyzer and (b) slow pyrolysis in fixed bed pyrolyzer. These two were chosen to account for the extremities of the process conditions. The contour plot for fast pyrolysis in fluidized bed is shown in **Figure 3**. The three vertices of the triangle are the maximum points of hemicellulose, cellulose, and lignin. For the minimization of gaseous products during fast pyrolysis in fluidized bed, the hemicellulose content in biomass is required to be high, when compared to the cellulose and lignin. More than 40% hemicellulose and  $\sim 20\%$  of each of lignin and cellulose in the biomass feed will minimize the gas yield during fast pyrolysis in fluidized bed. This is easily achievable, because there are biomasses with hemicellulose content higher than 40% (please refer to **Table 1**). Considering fast pyrolysis of wheat straw in fluidized bed reactor, which contains 25.5% hemicellulose, 49.3% cellulose, and 25.2% of lignin, the gas yield is  $\sim 30\%$ , which is consistent with the experimentally obtained data presented in **Table 3**.

The gas yield during slow pyrolysis in fixed bed pyrolysis is higher than that of fast pyrolysis in fluidized bed reactors. This is due to the fact that the residence time in the fixed bed reactors is higher when compared to that of fluidized bed reactors. Due to longer residence times, there are secondary reactions, that is, the conversion of liquid into gas and char. The optimal minimum gas yield during slow biomass pyrolysis in fixed bed reactors is  $\sim 16\%$ , as shown in contour plot in **Figure 4**. The minimum gas yield can be obtained at various conditions. Specifically, it is obtained either at high hemicellulose content or at medium cellulose and lignin content in the

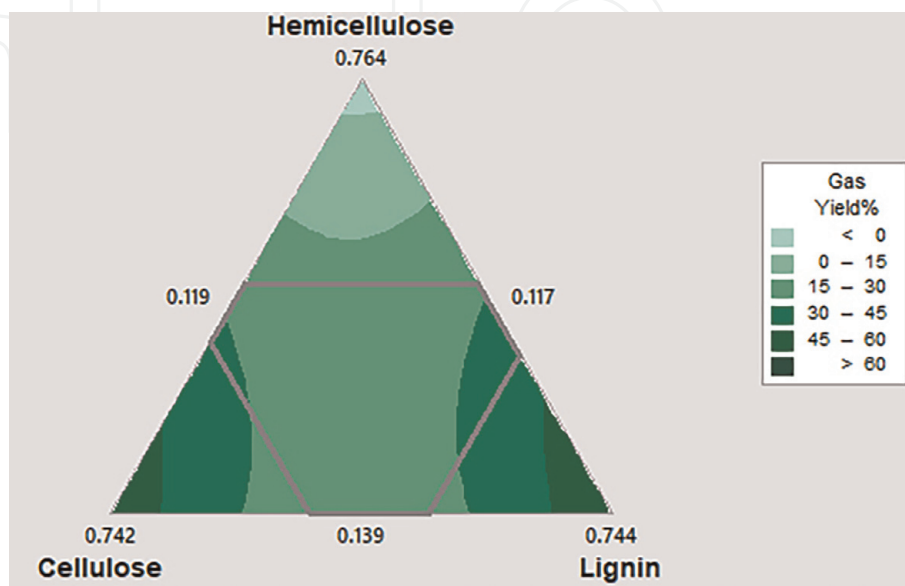


**Figure 3.**  
Contour plot of gas yield in biomass pyrolysis for fast pyrolysis in fluidized bed reactor.

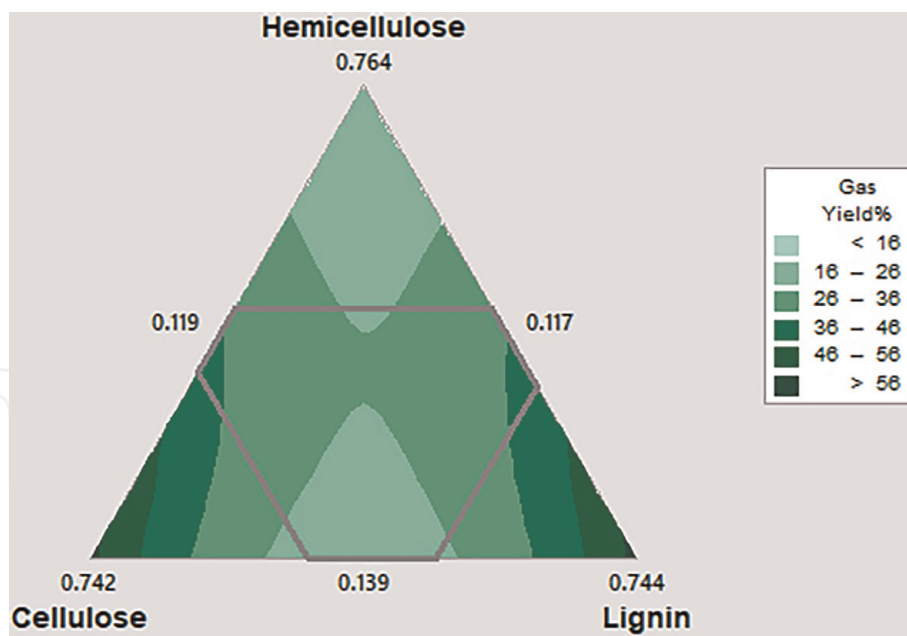


**Figure 4.**  
Contour plot of gas yield in biomass pyrolysis for slow pyrolysis in fixed bed reactor.

biomass. Considering the wheat straw decomposition during slow pyrolysis in fixed bed, the gas yield is 16–26% as given by **Figure 4**.

The gas yield during biomass pyrolysis may be obtained from statistical modeling, presented in Eq. (16). This equation was obtained after removing the model terms that were not statistically significant, that is, terms with  $p$ -value  $< 0.05$ .

$$\text{GasYield}(\%) = -20.4 * H + 108.8 * C + 111.3 * L - 377.8 * C * L - 18.3 * H * P + 50.1 * H * L * R \quad (16)$$

where  $H$  is the hemicellulose fraction in biomass;  $C$  is the cellulose fraction in biomass;  $L$  is the lignin fraction in biomass;  $P$  is the pyrolysis type (fast or slow);  $R$  is the reactor type (fluidized bed or fixed bed).

The coefficients present in Eq. (16) represents whether the effect is positive or negative. The coefficient for hemicellulose is negative. This means, the higher the hemicellulose content, lesser will be the gas yield. From Eq. (16), there are interactions between cellulose-lignin, hemicellulose-pyrolysis type and hemicellulose-lignin-reactor type. These interactions could be either synergistic (positive coefficient) or antagonistic (negative coefficient). For the gas yield%, the cellulose-lignin and hemicellulose-pyrolysis are antagonistic, whereas hemicellulose-lignin-reactor type is synergistic.

Equations similar to gas yield%, presented in Eq. (16) were also obtained for liquid yield% and char yield%.

### 5.3 Optimization of liquid yield

As mentioned in Section 5.1, it is important find the level of biomass constituents and operating conditions for pyrolysis to maximize the liquid yield, while minimizing both gas and char yield.

**Figure 5** presents the contour plot of liquid yield as function of biomass constituents during fast pyrolysis. The maximum liquid yield may be obtained at high hemicellulose, low lignin and low cellulose content. For biomasses whose cellulose content is high, the liquid yields are very low and for the biomasses whose lignin

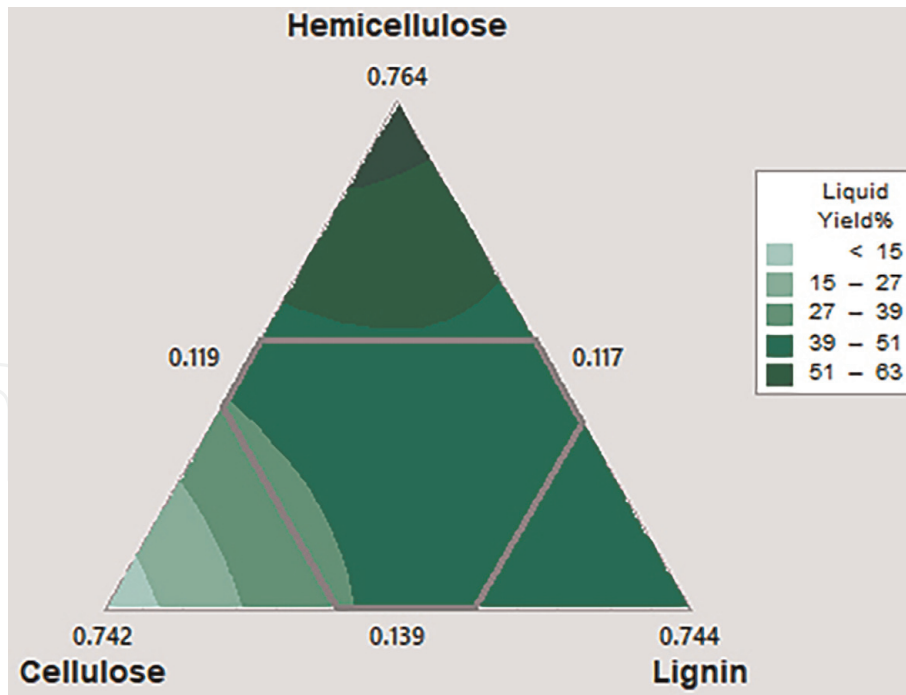


**Figure 5.**  
 Contour plot of liquid yield in biomass pyrolysis for fast pyrolysis in fluidized bed reactor.

content is high, the liquid yield ranges from 40 to 60%. For example, one of the biomasses containing high hemicellulose is switch grass, for which, if decomposed during fast pyrolysis in fluidized bed, the liquid yield is more than 51% (from **Figure 5**), which is consistent with the experimentally obtained data.

**Figure 6** shows the liquid yield during slow pyrolysis in fixed bed pyrolyzes. Comparing **Figure 5** with **Figure 6**, it can be concluded that, the liquid yield is higher in fast pyrolysis in fluidized bed than slow pyrolysis in fixed bed. Further, the maximum liquid yield that can be obtained is ~40%. This can be obtained only at high hemicellulose content, medium cellulose content and low lignin content. The liquid yield for the high hemicellulose content biomasses, such as switch grass,

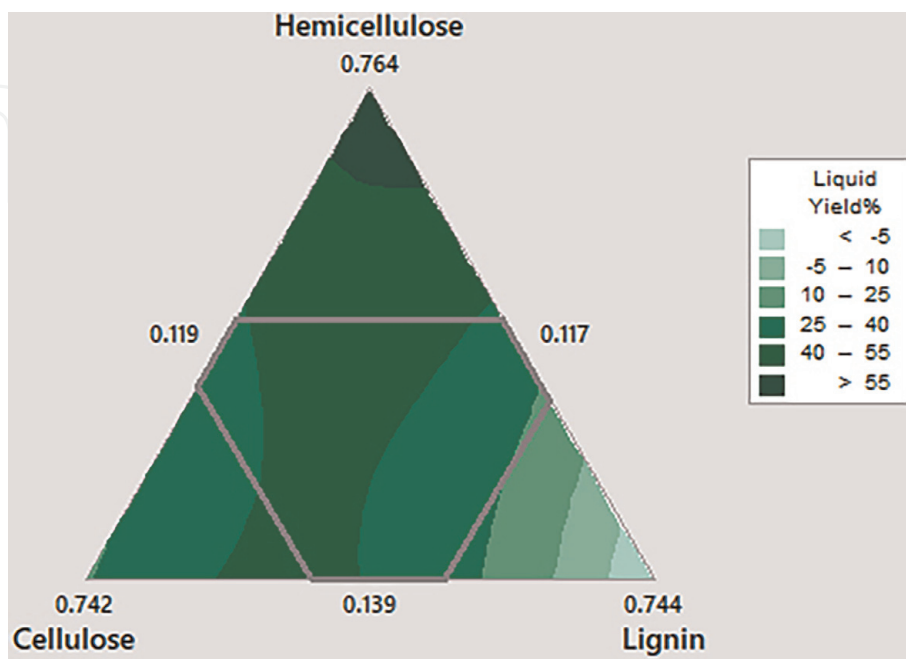


**Figure 6.**  
 Contour plot of liquid yield in biomass pyrolysis for slow in fixed bed reactor.

during slow pyrolysis in fixed bed reactor, the liquid yield will vary from 25 to 40%, which can be obtained from **Figure 6**.

#### 5.4 Optimization of char yield

Minimization of char is also important during biomass pyrolysis. **Figure 7** shows the contour plot of char yield during fast pyrolysis in fluidized bed and **Figure 8** shows the char yield during slow pyrolysis in fixed bed. Lower char yields may be

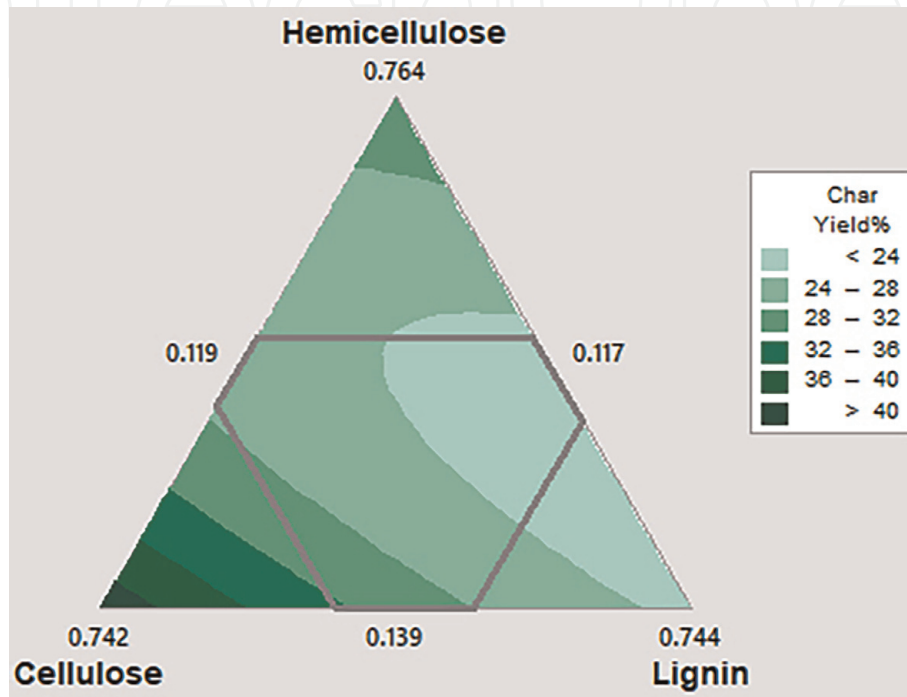


**Figure 7.**  
*Contour plot of char yield in biomass pyrolysis for fast pyrolysis in fluidized bed reactor.*

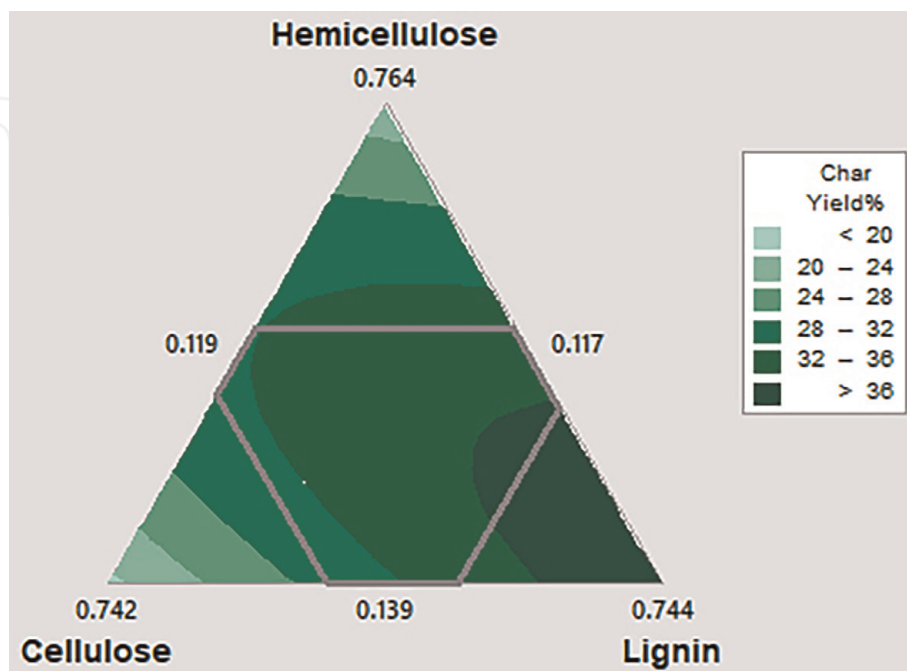


**Figure 8.**  
*Contour plot of char yield in biomass pyrolysis for slow pyrolysis in fixed bed reactor.*

obtained during fast pyrolysis in fluidized bed from biomasses containing higher amount of lignin, medium amounts of hemicellulose and lower amounts of cellulose (lignocellulosic biomass in other words). For example, the high lignin biomasses such as hazelnut shell will yield less char during fast pyrolysis in fluidized bed reactor.

Low char yields may be obtained for biomasses with high hemicellulose and high lignin during slow pyrolysis in fixed bed operation.

## **6. Conclusions**

Biomasses vary widely in their chief constituents namely, hemicellulose, cellulose, and lignin. The order of the degradation temperature for the three chief constituents is hemicellulose < cellulose < lignin. For obtaining controlled and useful product profiles such as liquid fuels via pyrolysis, it is important to understand the pyrolysis process conditions, such as heating rate and temperature. For optimization, the pyrolysis operating parameters are classified as slow and fast pyrolysis and the reactors are classified as fluidized bed and fixed bed. The data required for optimization was obtained from many sources, including experimental data for various biomasses and process conditions. The response surface optimization was performed using mixture design with three levels for biomass constituents and two levels each for pyrolysis type and reactor type. The objective of this book chapter is to model the reaction using lumped (gas, liquids, and char) approach and find the feed and operating parameters to maximize the liquid yield. In general, the liquid yield was found to be higher during fast pyrolysis/fluidized bed reactors when compared to slow pyrolysis/fixed bed reactors. This is due to the large residence time in the slow pyrolysis/fixed bed reactors. The maximum yield may be obtained for the biomasses containing high hemicellulose such as switch grass and corn stock.

The authors recommend further optimization with respect to particle size, heating rate, and biomass feed rate.

## **Acknowledgements**

The authors acknowledge the financial support from the Center of Excellence in Advanced Materials & Green Technologies, granted under the Frontier Areas of Science and Technology (FAST) scheme to establish the Centers of Excellence by Ministry of Human Resource Development (MHRD), Government of India.

## **Conflict of interest**

There is no conflict of interest.

## **Notes/Thanks/Other declarations**

The authors would like to thank the students who attended the course “Waste to Energy part of Masters in Materials Science and Engineering program, Amrita Vishwa Vidyapeetham,” who had helped in obtaining the data and supported the work through discussions.

IntechOpen

IntechOpen

### Author details

Udaya Bhaskar Reddy Ragula\*, Sriram Devanathan and Sindhu Subramanian  
Department of Chemical Engineering and Materials Science, Amrita Vishwa  
Vidyapeetham, Coimbatore, India

\*Address all correspondence to: [u\\_bhaskarreddy@cb.amrita.edu](mailto:u_bhaskarreddy@cb.amrita.edu)

### IntechOpen

---

© 2019 The Author(s). Licensee IntechOpen. This chapter is distributed under the terms of the Creative Commons Attribution License (<http://creativecommons.org/licenses/by/3.0>), which permits unrestricted use, distribution, and reproduction in any medium, provided the original work is properly cited. 

## References

- [1] Basu P. Biomass Gasification and Pyrolysis Handbook. Kidlington, Oxford, UK: Elsevier; 2010. DOI: 10.1016/B978-0-12-374988-8.00001-5
- [2] Raj T, Kapoor M, Gaur R, Christopher J, Lamba B, Tuli DK, et al. Physical and chemical characterization of various indian agriculture residues for biofuels production. *Energy & Fuels*. 2015;**29**:3111-3118. DOI: 10.1021/ef5027373
- [3] Dhyani V, Bhaskar T. A comprehensive review on the pyrolysis of lignocellulosic biomass. *Renewable Energy*. 2018;**129**:695-716. DOI: 10.1016/j.renene.2017.04.035
- [4] Jahirul MI, Rasul MG, Chowdhury AA, Ashwath N. Biofuels production through biomass pyrolysis—A technological review. *Energies*. 2012;**5**:4952-5001. DOI: 10.3390/en5124952
- [5] Braga RM, Melo DMA, Aquino FM, Freitas JCO, Melo MAF, Barros JMF, et al. Characterization and comparative study of pyrolysis kinetics of the rice husk and the elephant grass. *Journal of Thermal Analysis and Calorimetry*. 2014;**115**:1915-1920. DOI: 10.1007/s10973-013-3503-7
- [6] Uzun BB, Yaman E. Pyrolysis kinetics of walnut shell and waste polyolefins using thermogravimetric analysis. *Journal of the Energy Institute*. 2016;**90**:1-13. DOI: 10.1016/j.joei.2016.09.001
- [7] Räsänen T, Athanassiadis D. Basic chemical composition of the biomass components of pine, spruce and birch. *Forest Refine*. 2013;**3**:1-4
- [8] Guerrero MRB, Marques Da Silva Paula M, Zaragoza MM, Gutiérrez JS, Velderrain VG, Ortiz AL, et al. Thermogravimetric study on the pyrolysis kinetics of apple pomace as waste biomass. *International Journal of Hydrogen Energy*. 2014;**39**:16619-16627. DOI: 10.1016/j.ijhydene.2014.06.012
- [9] Özsin G, Pütün AE. Kinetics and evolved gas analysis for pyrolysis of food processing wastes using TGA/MS/FT-IR. *Waste Management*. 2017;**64**:315-326. DOI: 10.1016/j.wasman.2017.03.020
- [10] Chandrasekaran A, Ramachandran S, Subbiah S. Determination of kinetic parameters in the pyrolysis operation and thermal behavior of *Prosopis juliflora* using thermogravimetric analysis. *Bioresource Technology*. 2017;**233**:413-422. DOI: 10.1016/j.biortech.2017.02.119
- [11] Tsamba AJ, Yang W, Blasiak W. Pyrolysis characteristics and global kinetics of coconut and cashew nut shells. *Fuel Processing Technology*. 2006;**87**:523-530. DOI: 10.1016/j.fuproc.2005.12.002
- [12] Li LL, Fu XB, Wang XN, Tian YY, Qin S. Pyrolytic characteristics and kinetic studies of agricultural wastes—four kinds of grasses. *Energy Sources, Part A: Recovery, Utilization, and Environmental Effects*. 2016;**38**:1156-1162. DOI: 10.1080/15567036.2013.856967
- [13] Islam MA, Asif M, Hameed BH. Pyrolysis kinetics of raw and hydrothermally carbonized Karanj (*Pongamia pinnata*) fruit hulls via thermogravimetric analysis. *Bioresource Technology*. 2015;**179**:227-233. DOI: 10.1016/j.biortech.2014.11.115
- [14] Subramanian S, Ragula UBR. Pyrolysis kinetics of *Hibiscus rosa sinensis* and *Nerium oleander*. *Biofuels*. 2018;**7269**:1-15. DOI: 10.1080/17597269.2018.1432274

- [15] Vinodhini S, Malathy NS. Bioprospecting of plants fibre of Coimbatore district of Tamil Nadu. *International Journal of Plant Sciences*. 2009;**4**:444-445
- [16] Jabli M, Tka N, Ramzi K, Saleh TA. Physicochemical characteristics and dyeing properties of lignin-cellulosic fibers derived from *Nerium oleander*. *Journal of Molecular Liquids*. 2018;**249**: 1138-1144. DOI: 10.1016/j.molliq.2017.11.126
- [17] Suriapparao DV, Vinu R. Effects of biomass particle size on slow pyrolysis kinetics and fast pyrolysis product distribution. *Waste and Biomass Valorization*. 2017;**9**:1-13. DOI: 10.1007/s12649-016-9815-7
- [18] Gaston KR, Jarvis MW, Pepiot P, Smith KM, Frederick WJ, Nimlos MR. Biomass pyrolysis and gasification of varying particle sizes in a fluidized-bed reactor. *Energy & Fuels*. 2011;**25**: 3747-3757. DOI: 10.1021/ef200257k
- [19] Niu Y, Tan H, Liu Y, Wang X, Xu T. The effect of particle size and heating rate on pyrolysis of waste capsicum stalks biomass. *Energy Sources, Part A: Recovery, Utilization, and Environmental Effects*. 2013;**35**: 1663-1669. DOI: 10.1080/15567036.2010.509084
- [20] Tsai WT, Lee MK, Chang YM. Fast pyrolysis of rice straw, sugarcane bagasse and coconut shell in an induction-heating reactor. *Journal of Analytical and Applied Pyrolysis*. 2006;**76**:230-237. DOI: 10.1016/j.jaap.2005.11.007
- [21] Lignite M. Effects of heating rate and particle size on pyrolysis kinetics of mungen lignite. *Energy Sources*. 2001;**23**:337-344. DOI: 10.1080/009083101300110887
- [22] Basu P. Biomass Gasification and Pyrolysis: Practical Design and Theory. Kidlington, Oxford, UK: Academic Press; 2010. <https://doi.org/10.1016/C2009-0-20099-7>
- [23] Guerrero MRB, Salinas Gutiérrez JM, Meléndez Zaragoza MJ, López Ortiz A, Collins-Martínez V. Optimal slow pyrolysis of apple pomace reaction conditions for the generation of a feedstock gas for hydrogen production. *International Journal of Hydrogen Energy*. 2016;**41**:23232-23237. DOI: 10.1016/j.ijhydene.2016.10.066
- [24] Pratap A, Chouhan S. A slow pyrolysis of cotton stalk (*Gossypium arboretum*) waste for bio-oil production. *Journal of Pharmaceutical, Chemical and Biological Sciences*. 2015;**3**:143-149
- [25] Demirbas MF, Balat M. Biomass pyrolysis for liquid fuels and chemicals: A review. *Journal of Scientific and Industrial Research*. 2007;**66**:797-804
- [26] Polat S, Apaydin-Varol E, Pütün AE. Thermal decomposition behavior of tobacco stem. Part II: Kinetic analysis. *Energy Sources, Part A: Recovery, Utilization, and Environmental Effects*. 2016;**38**:3073-3080. DOI: 10.1080/15567036.2015.1129374
- [27] Raveendran K, Ganesh A, Khilar KC. Pyrolysis characteristics of biomass and biomass components. *Fuel*. 1996;**75**: 987-998
- [28] Greenhalf CE, Nowakowski DJ, Harms AB, Titiloye JO, Bridgwater AV. A comparative study of straw, perennial grasses and hardwoods in terms of fast pyrolysis products. *Fuel*. 2013;**108**: 216-230. DOI: 10.1016/j.fuel.2013.01.075
- [29] Vyazovkin S, Burnham AK, Criado JM, Pérez-Maqueda LA, Popescu C, Sbirrazzuoli N. ICTAC kinetics committee recommendations for performing kinetic computations on thermal analysis data. *Thermochimica Acta*. 2011;**520**:1-19. DOI: 10.1016/j.tca.2011.03.034

- [30] Kirubakaran V, Sivaramakrishnan V, Nalini R, Sekar T, Premalatha M, Subramanian P. A review on gasification of biomass. *Renewable and Sustainable Energy Reviews*. 2009;**13**:179-186. DOI: 10.1016/j.rser.2007.07.001
- [31] Williams PT, Besler S. The pyrolysis of rice husks in a thermogravimetric analyser and static batch reactor. *Fuel*. 1993;**72**:151-159. DOI: 10.1016/0016-2361(93)90391-E
- [32] El-Sayed SA, Mostafa ME. Pyrolysis characteristics and kinetic parameters determination of biomass fuel powders by differential thermal gravimetric analysis (TGA/DTG). *Energy Conversion and Management*. 2014;**85**: 165-172. DOI: 10.1016/j.enconman.2014.05.068
- [33] Mani T, Murugan P, Abedi J, Mahinpey N. Pyrolysis of wheat straw in a thermogravimetric analyzer: Effect of particle size and heating rate on devolatilization and estimation of global kinetics. *Chemical Engineering Research and Design*. 2010;**88**:952-958. DOI: 10.1016/j.cherd.2010.02.008
- [34] Shen J, Igathinathane C, Yu M, Pothula AK. Biomass pyrolysis and combustion integral and differential reaction heats with temperatures using thermogravimetric analysis/differential scanning calorimetry. *Bioresource Technology*. 2015;**185**:89-98. DOI: 10.1016/j.biortech.2015.02.079
- [35] Xiwen Y, Kaili X, Yu L. Assessing the effects of different process parameters on the pyrolysis Beha.: EBSCOhost. *Bio Resources*. 2017;**12**: 2748-2767. DOI: 10.1002/asi.22787
- [36] Collazzo GC, Broetto CC, Perondi D, Junges J, Dettmer A, Dornelles Filho AA, et al. A detailed non-isothermal kinetic study of elephant grass pyrolysis from different models. *Applied Thermal Engineering*. 2017;**110**:1200-1211. DOI: 10.1016/j.applthermaleng.2016.09.012
- [37] Ceylan S, Topçu Y. Pyrolysis kinetics of hazelnut husk using thermogravimetric analysis. *Bioresource Technology*. 2014;**156**:182-188. DOI: 10.1016/j.biortech.2014.01.040
- [38] Haykiri-Acma H, Yaman S. Synergy in devolatilization characteristics of lignite and hazelnut shell during co-pyrolysis. *Fuel*. 2007;**86**:373-380. DOI: 10.1016/j.fuel.2006.07.005
- [39] Wagenaar BM, Prins W, Swaaij WPM v. Flash pyrolysis kinetics of pine wood. *Fuel Processing Technology*. 1993;**36**:291-298
- [40] Özsın G, Pütün AE. Co-pyrolytic behaviors of biomass and polystyrene: Kinetics, thermodynamics and evolved gas analysis. *Korean Journal of Chemical Engineering*. 2018;**35**:428-437. DOI: 10.1007/s11814-017-0308-6
- [41] Gonzalez JF, Encinar JM, Canito JL, Sabio E, Chacon M. Pyrolysis of cherry stones: Energy uses of the different fractions and kinetic study. *Journal of Analytical and Applied Pyrolysis*. 2003; **67**:165-190
- [42] Fiori L, Valbusa M, Lorenzi D, Fambri L. Modeling of the devolatilization kinetics during pyrolysis of grape residues. *Bioresource Technology*. 2012;**103**:389-397. DOI: 10.1016/j.biortech.2011.09.113
- [43] Radmanesh R, Courbariaux Y, Chaouki J, Guy C. A unified lumped approach in kinetic modeling of biomass pyrolysis. *Fuel*. 2006;**85**:1211-1220. DOI: 10.1016/j.fuel.2005.11.021
- [44] Cao L, Yuan X, Jiang L, Li C, Xiao Z, Huang Z, et al. Thermogravimetric characteristics and kinetics analysis of oil cake and torrefied biomass blends. *Fuel*. 2016;**175**:129-136. DOI: 10.1016/j.fuel.2016.01.089
- [45] Tsai WT, Lee MK, Chang YM. Fast pyrolysis of rice husk: Product yields

and compositions. *Bioresource Technology*. 2007;**98**:22-28. DOI: 10.1016/j.biortech.2005.12.005

[46] Vieira FR, Luna CMR, Arce GLAF, Avila I. A study of biochar yield from slow pyrolysis of rice husk; In: 24th ABCM-Brazilian Association of Engineering and Mechanical Sciences; 2017. p. 1-6

[47] Ali N, Saleem M, Shahzad K, Chughtai A. Bio-oil production from fast pyrolysis of cotton stalk in fluidized bed reactor. *Arabian Journal for Science and Engineering*. 2015;**40**:3019-3027. DOI: 10.1007/s13369-015-1801-z

[48] Sidhu GK, Sandhya. Engineering properties of cotton stalks (*Gossypium hirsutum* L.), Indian. *Journal of Agricultural Research*. 2015;**49**:456-459. DOI: 10.18805/ijare.v49i5.5811

[49] Park J, Lee Y, Ryu C, Park Y. Slow pyrolysis of rice straw: Analysis of products properties, carbon and energy yields. *Bioresource Technology*. 2014; **155**:63-70. DOI: 10.1016/j.biortech.2013.12.084

[50] Song H, Andreas J, Minhou X. Kinetic study of Chinese biomass slow pyrolysis: Comparison of different kinetic models. *Fuel*. 2007;**86**:2778-2788. DOI: 10.1016/j.fuel.2007.02.031

[51] Mohanty P, Nanda S, Pant KK, Naik S, Kozinski JA, Dalai AK. Evaluation of the physiochemical development of biochars obtained from pyrolysis of wheat straw, timothy grass and pinewood: Effects of heating rate. *Journal of Analytical and Applied Pyrolysis*. 2013;**104**:485-493. DOI: 10.1016/j.jaap.2013.05.022

[52] Fu P, Li Z, Bai X, Altilia WY, Pietrangeli F, Torre AD, et al. Bio-oil production from fast pyrolysis of corn stalk in a fluidized bed. *Applied Mechanics and Materials*. 2014;

**672–674**:143-146. DOI: 10.4028/www.scientific.net/AMM.672-674.143

[53] Cordella M, Berrueco C, Santarelli F, Paterson N, Kandiyoti R, Millan M. Yields and ageing of the liquids obtained by slow pyrolysis of sorghum, switchgrass and corn stalks. *Journal of Analytical and Applied Pyrolysis*. 2013; **104**:316-324. DOI: 10.1016/j.jaap.2013.07.001

[54] Zhang H, Xiao R, Wang D, He G, Shao S, Zhang J, et al. Biomass fast pyrolysis in a fluidized bed reactor under N<sub>2</sub>, CO<sub>2</sub>, CO, CH<sub>4</sub> and H<sub>2</sub> atmospheres. *Bioresource Technology*. 2011;**102**:4258-4264. DOI: 10.1016/j.biortech.2010.12.075

[55] Demirbas A. Effects of temperature and particle size on bio-char yield from pyrolysis of agricultural residues. *Journal of Analytical and Applied Pyrolysis*. 2004;**72**:243-248. DOI: 10.1016/j.jaap.2004.07.003

[56] Sousa J, Bezerra M, Almeida M, Moure G, Mesa-Perez J, Caramao E. Characteristics of bio-oil from the fast pyrolysis of elephant grass (*Pennisetum purpureum* schumach) in a fluidized bed reactor. *American Chemical Science Journal*. 2016;**14**:1-10. DOI: 10.9734/ACSJ/2016/25843

[57] Boateng AA, Mullen CA, Goldberg N, Hicks KB, Jung HJG, Lamb JFS. Production of bio-oil from alfalfa stems by fluidized-bed fast pyrolysis. *Industrial and Engineering Chemistry Research*. 2008;**47**:4115-4122. DOI: 10.1021/ie800096g

[58] Strezov V, Evans TJ, Hayman C. Conversion of elephant grass (*Pennisetum purpureum* schum) to bio-gas, bio-oil and charcoal. *Bioresource Technology*. 2008;**99**:8394-8399. DOI: 10.1016/j.biortech.2008.02.039

[59] Koçkar ÖM, Onay Ö, Pütün AE, Pütün E. Fixed-bed pyrolysis of

- hazelnut shell: A study on mass transfer limitations on product yields and characterization of the pyrolysis oil. *Energy Sources*. 2000;**22**:913-924. DOI: 10.1080/00908310051128291
- [60] Carrier M, Hugo T, Gorgens J, Knoetze H. Comparison of slow and vacuum pyrolysis of sugar cane bagasse. *Journal of Analytical and Applied Pyrolysis*. 2011;**90**:18-26. DOI: 10.1016/j.jaap.2010.10.001
- [61] Chen T, Liu R, Scott NR. Characterization of energy carriers obtained from the pyrolysis of white ash, switchgrass and corn stover-biochar, syngas and bio-oil. *Fuel Processing Technology*. 2016;**142**: 124-134. DOI: 10.1016/j.fuproc.2015.09.034
- [62] Onay Ö, Beis SH, Koçkar ÖM. Pyrolysis of walnut shell in a well-swept fixed-bed reactor. *Energy Sources*. 2004;**26**:771-782. DOI: 10.1080/00908310490451402
- [63] Yuan HR, Liu RH. Study on pyrolysis kinetics of walnut shell. *Journal of Thermal Analysis and Calorimetry*. 2007;**89**:983-986. DOI: 10.1504/IJGEI.2008.018006
- [64] Suttibak S, Sriprateep K, Pattiya A. Production of bio-oil from pine sawdust by rapid pyrolysis in a fluidized-bed reactor. *Energy Sources, Part A: Recovery, Utilization, and Environmental Effects*. 2015;**37**: 1440-1446. DOI: 10.1080/15567036.2011.631091
- [65] Uzun BB, Kanmaz G. Effect of operating parameters on bio-fuel production from waste furniture sawdust. *Waste Management & Research*. 2013;**31**:361-367. DOI: 10.1177/0734242X12470402
- [66] Wang Z, Cao J, Wang J. Pyrolytic characteristics of pine wood in a slowly heating and gas sweeping fixed-bed reactor. *Journal of Analytical and Applied Pyrolysis*. 2009;**84**:179-184. DOI: 10.1016/j.jaap.2009.02.001
- [67] Sundaram EG, Natarajan E. Pyrolysis of coconut shell: An experimental investigation. *Journal of Engineering Research*. 2009;**6**:33. DOI: 10.24200/tjer.vol6iss2pp33-39
- [68] Mythili R, Venkatachalam P, Subramanian P, Uma D. Characterization of bioresidues for biooil production through pyrolysis. *Bioresource Technology*. 2013;**138**:71-78. DOI: 10.1016/j.biortech.2013.03.161
- [69] Mythili R, Subramanian P, Uma D. Biofuel production from *Prosopis juliflora* in fluidized bed reactor. *Energy Sources, Part A: Recovery, Utilization, and Environmental Effects*. 2017;**39**: 741-746. DOI: 10.1080/15567036.2016.1261205
- [70] Chandrasekaran A, Ramachandran S, Subbiah S. Modeling, experimental validation and optimization of *Prosopis juliflora* fuelwood pyrolysis in fixed-bed tubular reactor. *Bioresource Technology*. 2018;**264**:66-77. DOI: 10.1016/j.biortech.2018.05.013
- [71] Xu J, Qiao L. Mathematical modeling of coal gasification processes in a well-stirred reactor: Effects of devolatilization and moisture content. *Energy & Fuels*. 2012;**26**:5759-5768. DOI: 10.1021/ef3008745
- [72] Narataruksa P, Tungkamani S, Pana-Suppamassadu K, Keeratiwintakorn P, Nivitchanyong S, Hunpinyo P, et al. Conversion enhancement of tubular fixed-bed reactor for Fischer-Tropsch synthesis using static mixer. *Journal of Natural Gas Chemistry*. 2012;**21**:435-444. DOI: 10.1016/S1003-9953(11)60388-5
- [73] Wu J, Zhang H, Ying W, Fang D. Simulation and analysis of a tubular fixed-bed Fischer-Tropsch synthesis

reactor with co-based catalyst. *Chemical Engineering and Technology*. 2010;**33**: 1083-1092. DOI: 10.1002/ceat.200900610

[74] Kunii D, Levenspiel O. *Fluidization Engineering*. 2nd ed. Boston: Elsevier; 1991

[75] Ciesielczyk W, Iwanowski J. Analysis of fluidized bed drying kinetics on the basis of interphase mass transfer coefficient. *Journal of Drying Technology*. 2006;**24**:1153-1157

[76] Agarwal PK, Genetti WE, Lee YY. Drying and devolatilization of Mississippi lignite in a fluidized-bed. *American Chemical Journal*. 1984;**29**

IntechOpen